Ordered nano-scale domains in lithium niobate single crystals via phase-mask assisted all-optical poling

I.T. Wellington[*]*, C.E. Valdivia, T. J. Sono, C.L. Sones, S. Mailis and R.W. Eason*.

Optoelectronics Research Centre, University of Southampton, Highfield,

Southampton. SO17 1BJ. U.K.

*Corresponding author: itw@orc.soton.ac.uk

Abstract

We report the formation of directionally-ordered nanoscale surface domains on the +z face of undoped congruent lithium niobate single crystals by using UV illumination through a phase mask of sub-micron periodicity with an energy fluence between ~90 mJ/cm^2 and 150 mJ/cm^2 at λ=266 nm. We clearly show here that the UV-induced surface ferroelectric domains only nucleate at and propagate along maxima of laser intensity. Although the domain line separation varies and is greater than 2μm for this set of experimental conditions, this enables a degree of control over the all-optical poling process.

PACS: 77.84.Dy, 81.65.Cf

Keywords: Lithium niobate, Ferroelectric domain inversion, Chemical etching,

Introduction

Fabrication of periodically inverted domain patterns in ferroelectric materials such as lithium niobate and lithium tantalate has been widely researched for the realization of applications as diverse as quasi-phase-matched (QPM) non-linear devices, electro-optic Bragg deflectors, photonic band-gap structures, and piezoelectric devices such as micro-resonators, atom traps and micro-cavities. While several techniques such as Li_2O out-diffusion [1], proton-exchange followed by heat treatment [2], Ti-indiffusion [3], scanning force microscopy [4], e-beam [5,6] and electric field poling [7] have successfully demonstrated domain inversion in lithium niobate crystals over the past few years, even the most routinely used technique of electric-field-induced domain inversion (E-field poling) becomes problematic when periodicities of a few microns and below are required for first-order QPM non-linear processes at blue to near-ultraviolet wavelengths.

To overcome the limitations associated with E-field poling, the technique of light-assisted E-field poling (LAP) which takes advantage of the ultraviolet light-induced transient change in the coercive field of the illuminated ferroelectric material has been developed during the past few years for lithium tantalate [8,9] and lithium niobate [10,11,12] crystals. Similar LAP experiments that use high intensity visible laser light, which has the effect of reducing the coercive field through a light-induced space charge field, have recently demonstrated directly written domain structures of ~2 μm width in undoped lithium niobate [13] and ~2 μm overall size in doped lithium niobate [14] samples.

Furthermore, an even simpler method for surface domain inversion has been investigated recently. This method exploits the interaction of intense ultraviolet laser light with ferroelectric lithium niobate to fabricate inverted ferroelectric domains of sub-micron width and few micron separation [15]. The resulting all-optically poled (AOP) ferroelectric domains, as described in reference 15, nucleate randomly within the irradiated laser spot and propagate preferentially along the principal crystal symmetry directions. Of course, for any practical application it is necessary to have control over the nucleation and propagation of the ferroelectric domains using such a method.

In this paper it is shown that it is indeed possible to impose a degree of control in the alignment of these UV-induced surface domains by illuminating with a spatially modulated UV laser beam. More specifically it is shown that it is possible to obtain ordered and aligned surface domains on the +z face of the crystal via an intensity pattern produced from a phase mask. The characterization of the laser-modified crystals and the domain nature was investigated using hydrofluoric acid etching of the UV exposed surface.

Experimental Procedure

The undoped congruent lithium niobate crystal samples were cut from z-cut optically polished, 500 μm thick wafers obtained from Crystal Technology, USA. The +z face was illuminated by two different pulsed UV laser sources to investigate wavelength sensitivity. The first laser was a frequency-quadrupled Nd:YVO_4 operating at $\lambda = 266$ nm with up to ~5 mJ pulses of ~10 ns duration. The second laser system was a frequency-doubled dye laser (Continuum Powerlite 8000) pumped by a frequency-

doubled Q-switched Nd:YAG laser. The dye laser system was tuneable from 289 nm to 329 nm, producing 0.5-1.5 mJ pulses of ~7 ns duration. Although this degree of tuneability was in principle an advantage that enabled exposure around the UV absorption edge of $LiNbO_3$, the laser output proved to have a highly inhomogeneous beam profile with undesirable local intensity variations. For this reason an aperture was used in an attempt to select an acceptably uniform area of the beam. Two different phase-masks, both with a period of 726 nm, were used for the UV laser exposures, optimized for $\lambda = 266$ nm and $\lambda = 298$ nm respectively. The experimental results and subsequent analysis suggested that the effect was essentially insensitive to the UV wavelength used (266 nm and 298 nm). However, due to the better beam quality of the frequency-quadrupled Nd:YVO_4 laser, the results corresponding to 266 nm exposures were mainly used for statistical analysis.

The phase mask was carefully aligned so that the grating lines would be parallel to one of the y-axes of the lithium niobate crystal, thereby ensuring preferential y-axis illumination and hence an increase in the probability for the optically induced ferroelectric inversion to occur along this particular axis. The phase mask was separated from the sample by two spacers consisting of two sections of standard telecom optical fibres having a diameter of 125 μm.

Single and multi-pulse (up to 10 pulses) exposures at 266 nm, over a wide range of fluences (between 5 and 200 mJ/cm^2), were performed on crystal samples and compared with samples exposed under the same conditions but without the phase-mask. After illumination, the UV exposed sample surface was etched for 20 minutes

in 48% hydrofluoric acid (HF) and inspected with optical and scanning electron microscopy (SEM).

Results and discussion

Initial experiments were conducted to establish the single pulse ablation threshold for the +z face of lithium niobate samples at both laser wavelengths. It is important to note at this point that AOP occurs near the ablation threshold. The single pulse ablation thresholds for 266 nm and 298 nm light were established experimentally to be between 95-105 mJ/cm^2. However, these figures are subject to some degree of uncertainty due to the intrinsic spatial non-uniformity and temporal (pulse to pulse) fluctuation of the dye laser. As with typical material ablation studies, these thresholds were observed to decrease for multi-pulse exposures.

Areas irradiated through the phase-mask at fluences significantly below the ablation threshold showed no evidence of domain formation. There exists, however, a narrow range of fluences (~90-150 mJ/cm^2) between which domain formation parallel to the phase-mask lines is possible with some degree of ablation damage. Considerably above the ablation threshold for a single pulse, weak domain formation was also observed, but it was accompanied by a pronounced ablation grating. Nevertheless, it is rather easy to distinguish between the laser damage pattern as subsequently revealed by the chemical etching and the ferroelectric pattern because etched ferroelectric domains are deeper and sharper than the ablated trenches.

The effect of UV illumination without the use of phase mask is shown in figure 1a. Here an SEM scan of the irradiated surface after HF acid etching is presented showing

the random nucleation and propagation of photo-induced domains along the three equivalent symmetry directions of the crystal. This effect has been extensively discussed before in reference [15]. Figure 1b shows an SEM image of the crystal surface that has been irradiated using a phase mask. The difference between these two images is readily apparent. Figure 1b shows that the majority of the photo-induced domains are aligned along a specific y-axis (vertical in the figure), dictated by the orientation of the phase mask which coincides with one of the crystal symmetry axes as shown in the inset direction indicator (top right). This was expected as the AOP domains nucleate only in the presence of near damage threshold optical intensity and propagate along the symmetry directions. In this experiment there is light only along a specific symmetry direction where the AOP domains are encouraged to nucleate and propagate resulting in the direction preference observed.

However, careful investigation of this domain formation details shows that the effect is more complex than initially expected. The SEM image presented in Figure 2 shows a magnified section of figure 1b. Although the domain lines formed are parallel to the phase mask lines, it is clear that the periodicity imposed by the phase mask ($\Lambda = 0.726$ μm) has not been faithfully reproduced in the resultant domain spacing. While measured domain widths are again in the range from 200-700 nm, the distance between them varies between ~2 μm and ~9.4 μm. This behaviour appears to underlie all such AOP experiments performed to date.

Imposition of a spatially extended light pattern with sub-micron periodicity, such as from the phase mask, appears to be opposed by the physical mechanism responsible for AOP. This is suggestive of an electrostatic mechanism, as the photo-generated

surface charge, likely to occur at the highly UV-absorbing surface, will result in electrostatic repulsion and re-organisation (e.g. clustering around surface defects). This imposes a characteristic electrostatic interaction length that overrides the imposed periodicity of the intensity pattern as the material is unable to both nucleate and sustain such closely packed domains via a strictly AOP process only. Another interesting observation can be made in figure 2 which also suggests electrostatic interaction between individual domains, namely that the domain lines produced are not continuous, but consist of irregular sections along the y-axis direction which is suggestive of correlated nucleation in highly non-equilibrium domain inversion reported in [16].

Of interest is the difference between apparently straight domain patterning at approximate values of 10Λ, and irregular domain lines that develop between them, as can also be seen in figure 2. This observation indicates that the initial conditions such as the sequence of nucleation and propagation of the domains are important. One possible explanation for the formation of the irregular domain lines between the straight lines could be that they were developed under the electrostatic influence of the previously formed straight lines.

Further investigation of the surface topography suggests that local intensity level variations significantly affect the AOP domain formation. Since there are variations of the local intensity across the laser spot (e.g. from the centre to the edge), different parts of the illuminated surface correspond to different conditions for nucleation and propagation of the photo-induced domains. In the case of Figure 2, AOP domains are

observed without the presence of ablation, hence indicating that ablation is not a necessary requirement for AOP.

The varying intensity profile across the laser beam allows investigation of the effect of local intensity variation on the AOP domain development. Figure 3 shows a part of the etched surface corresponding to the edge of an irradiated area exposed through a phase mask, and therefore experienced a slightly lower fluence. The area was illuminated with two pulses at $\lambda = 298$ nm at a fluence of ~160 mJ/cm^2. It becomes immediately clear after observing the SEM image (figure 3) that nucleation, and occasional limited subsequent propagation of domains, occurs only at positions of maximum light intensity. For this specific local exposure condition, simultaneous nucleation of sub-micron domains (top left) was obtained which are located in close proximity, even on adjacent phase mask intensity maxima. An area where both nucleation and growth (propagation) occur can also be observed in the same figure (bottom right), however these expanded domains are spaced further apart, resembling the situation shown in figure 2 where the domain lines maintain a distance of 3.6-7.2 μm.

In a subsequent experiment the phase-mask was rotated so that the grating lines were at an angle of approximately 38° with respect to the crystallographic y-axis of the exposed sample. The purpose of this experiment was to conclude whether the crystal symmetry prevails over the spatial modulation of the optical intensity pattern, in other words to show whether arbitrarily-aligned domain patterns can be produced. In this experiment a single 266 nm pulse of fluence ~150 mJ/cm^2 was applied to generate a clearly visible ablation grating which was used to identify the rotation angle.

Investigation of the surface topography after etching showed that it is not possible to override the symmetry directions of the crystal. As in all previous cases the AOP domains nucleate on the maxima of the optical intensity but they cannot be encouraged to propagate along the direction imposed by the optical intensity distribution unless this direction coincides with one of the y-axes of symmetry. Figure 4 shows a detailed SEM scan of the HF-etched surface where the ablation grating is clearly visible and the y-axis directions are indicated in the inset diagram (top left). Investigation of figure 4 confirms the earlier statement that sub-micron (~300 nm) AOP domains are located on the maxima of the optical intensity pattern but they can only propagate along the y-directions which in this case is not possible due to the absence of light in the "dark" fringes of the illuminating optical intensity pattern produced by the phase mask.

However, it is interesting to note that individual adjacent domains are aligned along these three y-directions of the crystal at a fixed period imposed by the intensity pattern. Hence it may be possible to have dense packing of periodic domains along the "y" symmetry directions, for example, by 2D periodic illumination.

As noted previously, all optical ferroelectric domain reversal occurs only at the maxima of the laser intensity distribution as produced by the phase-mask. However, the separation between adjacent domains, although always a multiple of the phase mask period, is variable. A systematic study of the domain separation along the x-axis was performed on samples fabricated using a range of laser fluences (~100 – ~150 mJ/cm^2). This study revealed that the distribution of domain separation does not

depend on the laser energy fluence. The observed separation distributions have shown a maximum of 10% deviation from the average domain separation across this range of fluences, with no difference between single or double-pulse exposures.

The average of domain separation distribution over different samples is shown in the histogram of figure 5. This histogram indicates that 88% of the measured domain separation widths lie between 4Λ - 8Λ (2.9 μm- 5.8 μm). Significantly, as shown in the histogram there are no separations between domain lines under 3Λ (2.18 μm), underlining the hypothesis of a minimum domain formation distance.

The effect of temperature on the formation of AOP domains was also investigated by a simple experiment. The crystal/phase mask assembly was placed on a hot plate, and exposures were performed at different equilibrium temperatures ranging from room temperature to 200°C. No qualitative difference was observed at temperatures below 100°C. However as the temperature increased, it was observed that the domain density is significantly reduced and domain lines tend to develop even further apart than in the room temperature case. The major difference is that the domain lines do not consist of individual sections but form continuous lines. Figure 6 shows an SEM micrograph of continuous domain lines as a result of irradiation at a temperature of 190°C.

All the experimental results so far have not been able to provide a conclusive physical interpretation of the effect. Nevertheless there are numerous indications suggesting that the AOP process originates from charge imbalance which is the result of the removal of surface charge compensating crystal layers via ablation. Other effects such

as Li_2O out-diffusion or side diffusion, the pyroelectric and piezoelectric effect which occur upon absorption of an intense UV pulse and subsequent rapid temperature rise may also contribute to the formation of AOP domains [17].

Conclusions

Ordered alignment of AOP domains has been achieved by spatially modulated UV laser radiation using a phase mask. The pulsed UV laser-induced domains nucleate on optical intensity maxima and are encouraged to grow along a specific "y" direction of the crystal specified by the aligned orientation of a periodic optical intensity pattern. However, full replication of the optical periodic pattern was not achieved due to possible electrostatic repulsion between adjacent domains which limits the minimum distance between them to ~2 μm for the range of illumination conditions used in our experiments.

Furthermore, for experiments performed at room temperature the ordered domain lines consist of discrete smaller domains, while at higher temperatures domain lines are continuous but tend to grow even further apart from each other. Experimental results suggest that although long domain lines cannot grow in close proximity due to electrostatic limitations, it may be possible to achieve denser packing of individual domains (domains which have just nucleated but not expanded) by illuminating with a 2D periodic intensity pattern.

Further work is required for the complete understanding of the physical mechanism behind this very interesting effect. The investigation which is presented here is an

important first step towards successful manipulation and control of AOP ferroelectric domains in congruent lithium niobate.

Acknowledgements

The authors are grateful to the Engineering and Physical Sciences Research Council (EPSRC) for research funding via grant EP/C515668/1 and to Dr Ian Clark and the Rutherford Appleton Central Laser Facility for the Continuum Powerlite 8000 dye laser loan.

References

1. K. Yamamoto, K. Mizuuchi, K. Takeshige, Y. Sasi, and T. Taniuchi, J. Appl. Phys. **70(4)**, 1947, (1991)
2. K. Nakamura, and H. Shimizu, Appl. Phys. Lett. **56(16)**, 1535, (1990)
3. S. Miyazawa, J. Appl. Phys. **50(7).** 4599, (1979)
4. K. Terabe, M. Nakamura, S. Takekawa, K. Kitamura, S. Higuchi, Y. Gotoh, and Y. Cho, Appl. Phys. Lett. **82 (3)**, 433, (2003)
5. M. Yamada, and K. Kishima, Electron. Lett. **27(10)**, 828, (1991)
6. H. Ito, C. Takyu, and H. Inaba, Electron. Lett. **27(14)**, 1221, (1991)
7. M. Yamada, N. Nada, M. Saitoh, and K. Watanabe, Appl. Phys. Lett. **62(5)**, 435, (1993)
8. S. Chao, W. Davis, D. D Tuschel, R. Nichols, M. Gupta, and H. C Cheng, Appl. Phys. Lett. **67**, 1066, (1995)
9. P. T Brown, G. W Ross, R. W Eason, and A. R Pogosyan, Opt. Commun. **163(4-6)**, 310, (1999)
10. M. Müller, E. Soergel, and K. Buse, Appl. Phys. Lett. **83(9)**, 1824, (2003)
11. A. Fujimura, T. Sohmura, and T. Suhara, Electron. Lett, **39 (9)**. 719, (2003)
12. M. C. Wengler, B. Fassbender, E. Soergel, and K. Buse, J. Appl. Phys. **96**, 2816, (2004)
13. V. Dierolf, and C. Sandmann, Appl. Phys. Lett. **84(20)**, 3987, (2004)
14. C. L. Sones, M. C. Wengler, C. E. Valdivia, S. Mailis, R. W. Eason, and K. Buse, Appl. Phys. Lett. **86(21)**, 212901 (2005)
15. C. E. Valdivia, C. L. Sones, J. G. Scott, S. Mailis, R. W. Eason, D. A. Scrymgeour, V. Gopalan, T. Jungk, E. Soergel, and I. Clark, Appl. Phys. Lett. **86(2)**, 022906, (2005)

16. V. Ya. Shur, “Correlated nucleation and self-organized kinetics of ferroelectric domains” in Nucleation Theory and Applications, J. W. P. Schmelzer, Wiley, 178-214, (2005)
17. K. Nakamura, H. Ando, H. Shimizu, Appl. Phys. Lett. **50(20)**, 1413, (1987)

List of figures

Figure 1: SEM micrographs of the etched +z face following a) illumination with a non-spatially-modulated beam, and b) illumination via a phase mask. The three symmetrical y-axes are indicated on the top right of the figure. Both exposures were performed with the frequency-quadrupled Nd:YVO_4 laser at $\lambda = 266$ nm, with energy fluence values above the threshold for ablation.

Figure 2: High magnification SEM micrograph of aligned discrete domain patterned region within the central area of a sample exposed via a phase mask at a laser fluence of ~100 mJ/cm^2 without observable surface damage. The directions of the y axes are indicated on the top right.

Figure 3: SEM micrograph taken at the edge of the phase mask irradiated area using λ=298 nm. The directions of the y axes are indicated on the top right.

Figure 4: SEM micrograph of the +z face illuminated through a phase mask which has been misaligned with respect to a y-axis by ~38°. The three "y" directions are indicated on the top left of the figure.

Figure 5: Histogram showing the occurrence probability of different domain separation widths, normalized to the period of the phase mask (PM). The data shown here are the average of measurements performed on samples produced with a range of laser fluences (~100 mJ/cm^2 - ~150 mJ/cm^2).

Figure 6: SEM micrograph of +z face illuminated through a phase mask with single 266 nm pulse (~110 mJ/cm^2) at a sample temperature of 190°C. The directions of the y axes are indicated on the top left**.**

Fig 1a.

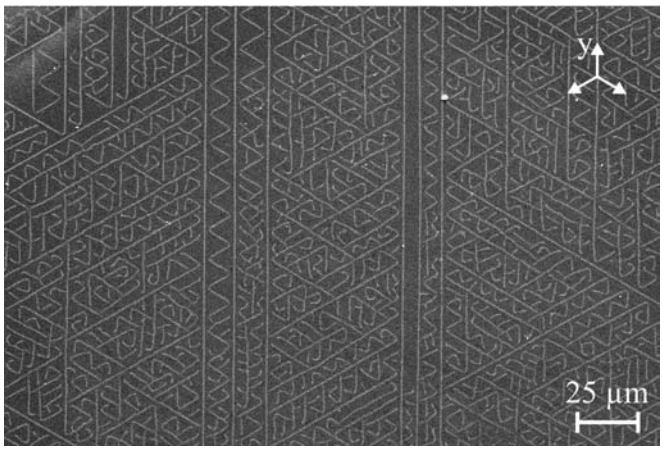

Fig 1b.

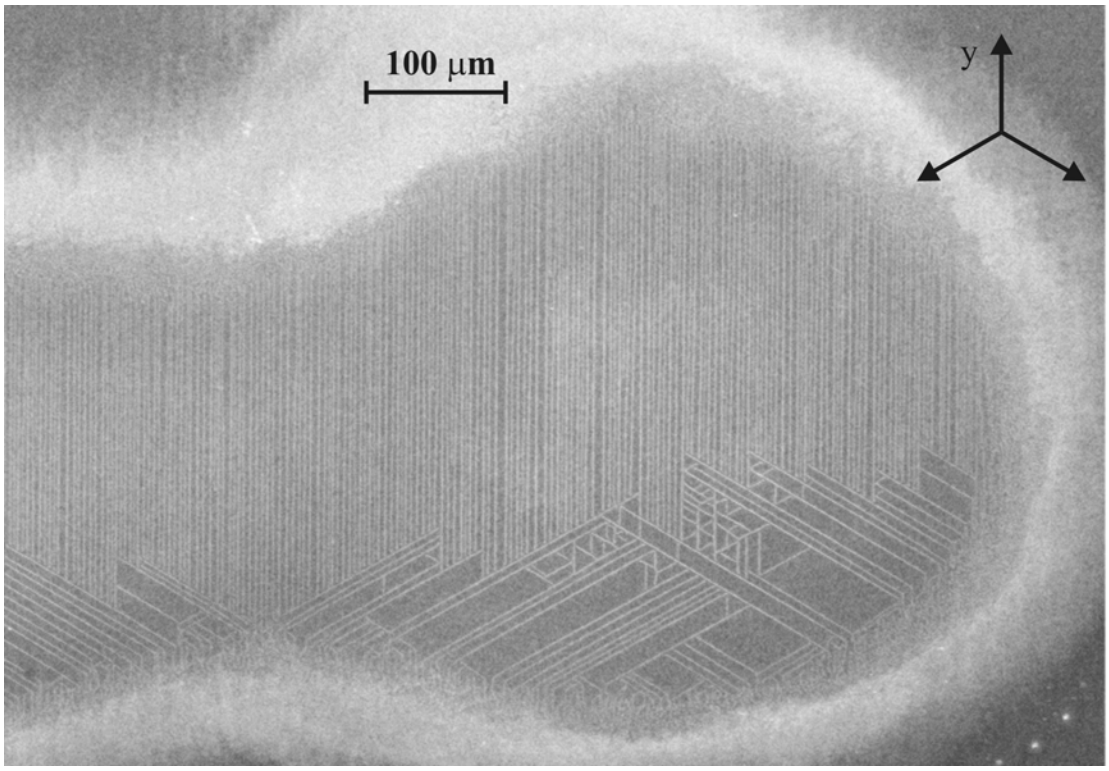

Fig 2.

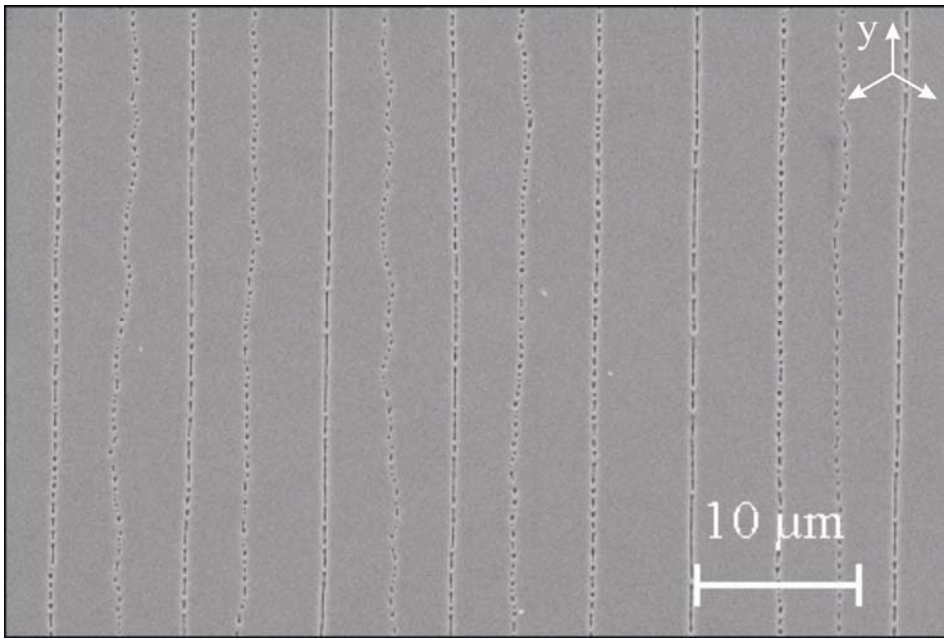

Fig 3.

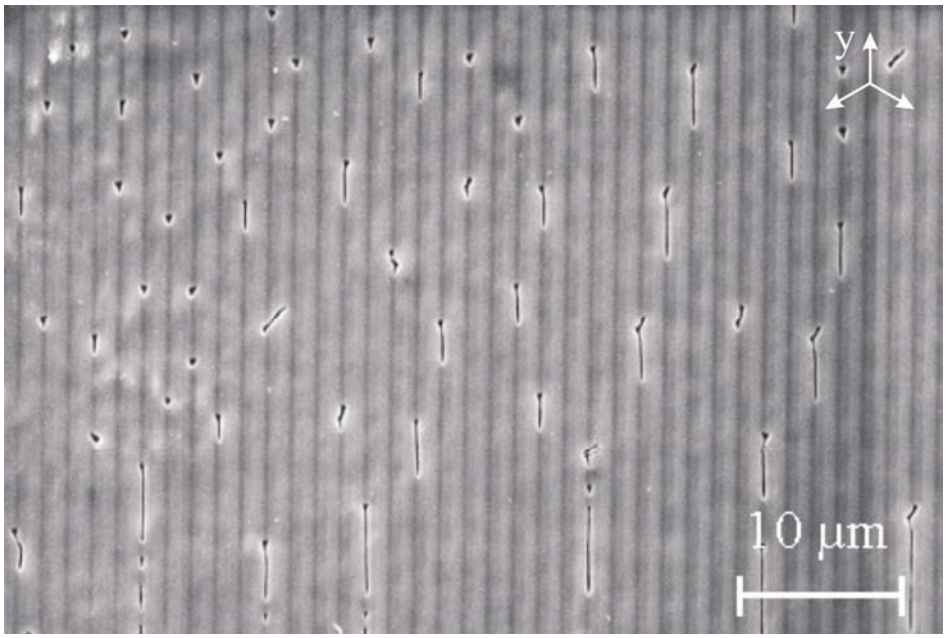

Fig 4.

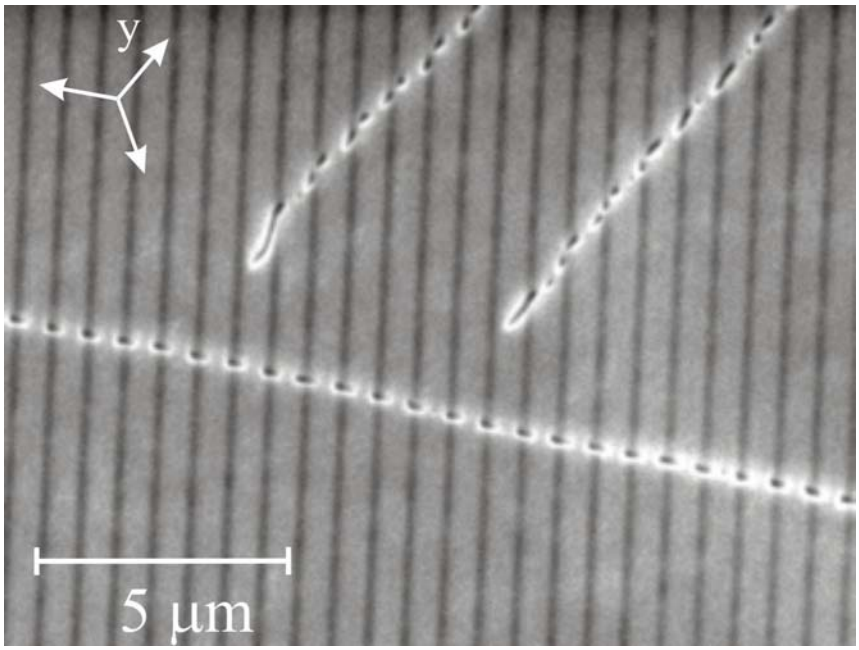

Fig 5.

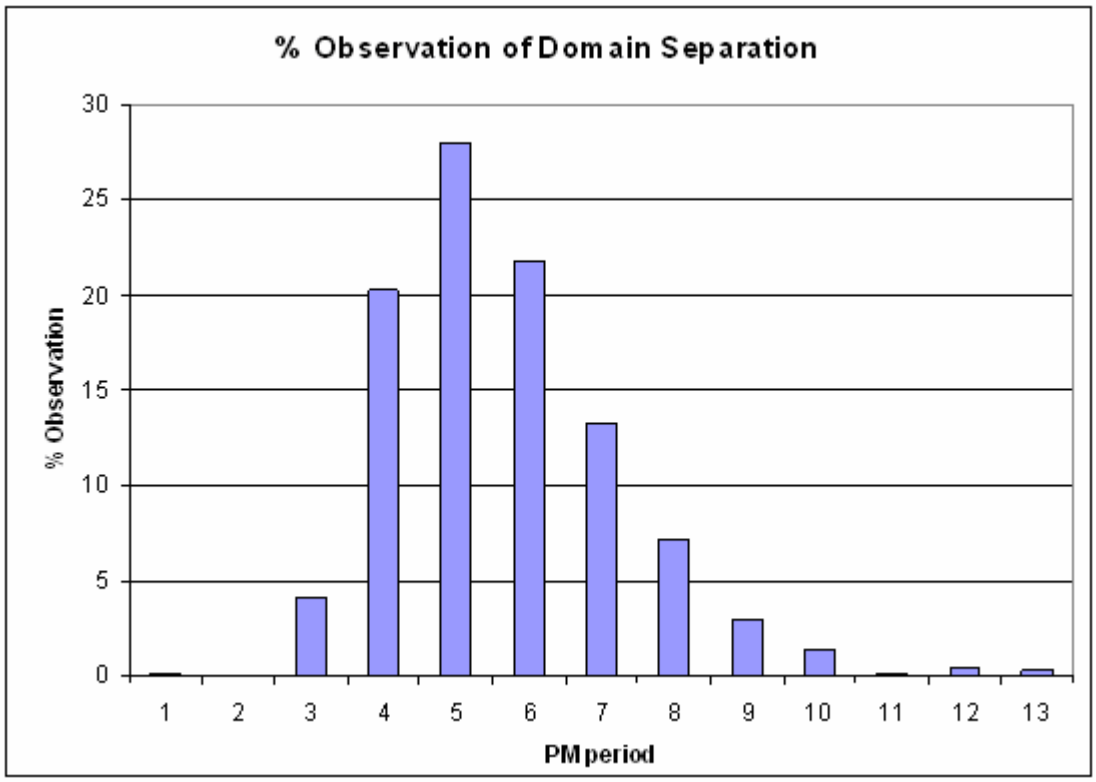
% Observation of Domain Separation
% Observation
30
25
20
15
10
5
0
1
2
3
4
5
6
7
8
9
10
11
12
13
PM period

Fig 6.